ISSN 2354-9114 (online), ISSN 0024-9521 (print)
Indonesian Journal of Geography Vol 57, No.1 (2025): 166-179
DOI: 10.22146/ijg.96393 website: https://jurnal.ugm.ac.id/ijg

INDONESIAN JOURNAL OF GEOGRAPHY

RESEARCH ARTICLE

Temperature and Climate Dynamics in National Capital Region of India

[1]Areesha, [2,3*]Pankaj Chauhan, [1]Rizwan Ahmed, [4]Sanjukta Bhaduri, [5]Dharmaveer Singh, [6]Md Kaikubad Ali

[1] Interdisciplinary Department of Remote Sensing and GIS Applications, AMU, Aligarh-202002, India
[2]Department of Glaciology and Environmental Geology, Wadia Institute of Himalayan Geology, Dehradun-248001, India
[3]Academy of Scientific and Innovative Research (AcSIR), Ghaziabad, India-201002
[4]School of Planning and Architecture, Delhi-110002, India
[5] Department of Geo-informatics, Symbiosis International (Deemed University), Pune-412115, India
[6]Department of Geography, Jamia Millia Islamia, New Delhi, Delhi 110025

Received: 2024-05-22 **Revised:** 2025-03-02**Accepted:** 2025-04-04 **Published:** 2025-04-28

Key words: Climate variability; Climate change; Global warming; UHI; LST; Geospatial approaches

Correspondent email : pchauhan1008@gmail.com

Abstract. Climate change and increase in global surface temperature are growing concerns worldwide, especially big urban agglomerations like National Capital Region of India, New Delhi and surrounding region have experienced exponential urbanization paving way to horizontal spilling of urban built-up areas, which consequently amplified the climate variability and surface temperature change over the past few decades. Therefore, the city is highly susceptible to several climate extremes, including heat waves, cold waves, droughts, and floods, impacting socioeconomic lives of over 20 million population. In this study, we applied remote sensing and GIS approaches to study climate variability and its impacts on urban areas. Indicators such as the Land Surface Temperature (LST), Urban Heat Islands (UHI), Normalized Difference Vegetation Index (NDVI), and Land Use Land Cover (LULC), were calculated using satellite data for the years 1993, 2000, 2010, and 2020. The result shows that LST values sharply rose as the maximum value reached 6.9°C in the last three decades (1993-2020), and UHIs maximum values reached 1.76, indicating a clear warming trend in the study area. During this period, the NDVI levels have decreased considerably, going from 0.59 to 0.21, which can be attributed to the expanding urbanization and the decreased green area. The LULC loss and gain analysis revealed that the urban area has rapidly expanded. In contrast, it resulted in loss of agricultural land, barren and scrubs, water bodies and forest area. The results show vast climate variability in the region posing threat to environment and socio-economic livelihood of the population.

1. Introduction

The availability of long-term climate records that help in understanding historical climate variability and its effects is limited in the challenging landscape (Rastogi et al., 2023) ('IMD | Environmental Monitoring Services', n.d.). Urban expansion, especially the horizontal spilling of built-up areas to accommodate the growing population, is closely associated with climate change and its adversaries (Pramanik & Punia, 2020). It emphasizes the need for the analysis of long-term climate records to comprehend historical climate variability. This variability refers to the fluctuations in meteorological parameters over time scales ranging from months to decades to centuries. According to (Wu et al., 2009), the hydrological cycle is anticipated to accelerate as an outcome of global warming. Climate change will inevitably cause climatic extremes, such as precipitation to increase (Chauhan et al., 2017). The speed of the montane hydrological systems can be increased due to warming-induced increases in plant activity and cover (Singh et al., 2021). River circulation patterns in the Himalayan region have altered due to rising temperatures and unpredictable rainfall brought on by climate change (Singh et al., 2023). Numerous variables can contribute to this variance, including changes in solar radiation, volcanic eruptions, ocean currents, and atmospheric circulation patterns (O'Malley et al., 2015). Long-term climate data will help to comprehend previous climatic variability and its influence. Comprehending the urban climate's unpredictability and the challenging Himalayan terrain region is important (Rastogi et al., 2023).

Urbanization-induced rapid land use/land cover change (LULCC) modifies the thermal characteristics of a region at the local scale and often creates urban heat island (UHI) effects (Pramanik & Punia, 2020).Built places are often hotter than the rural areas that surround them(Oke, 1982) . This phenomenon, often known as the "urban heat island effect," impacts several public health-related problems (Hsu et al., 2021). Climate variability has become a growing concern for urban centres worldwide, including New Delhi. Numerous research on changes in the climate in New Delhi has revealed an upward tendency in temperature and a downward trend in precipitation. In close proximity to the measurement device (usually measured in Kelvin), the crustal temperature of the earth at which absorption, reflection, and refraction of solar heat and radiation is known as LST. It is a significant aspect in a variety of fields, including heat balance research, urban land

use/cover, climate change, and many others. It is also a crucial input for climate models (Li et al., 2023). According to (Raja et al., 2018), sensible heat flux changes are closely related to the daily variation in mean land-air temperature differential, wind speed, and wind direction. In recent years, land-climate interfaces have come to be recognized as important forces on a regional and local level (Singh et al., 2022).

Satellite imagery offers incredibly valuable information that can be examined and manipulated to get credible outcomes (Gašparović & Singh, 2023); high resolution satellite and modelled data is crucial of water consumption and water resources management (Singh et al., 2023). Remote sensing studies of terrestrial dynamics now have several opportunities thanks to LANDSAT data. LST varies with changes in weather conditions and other human activity, making precise prediction difficult (Singh et al., 2021). While some academics contend that cities are entirely capable of adapting to it, urbanization has a direct impact on climate change. Due to the concurrent alteration of natural landscape and incorporation of built-up elements, i.e., anthropogenic surfaces, globalization has greatly escalate greenhouse gases and changed the landscape, which has profound climatic ramifications at every scales(M & Babu, 2018).The identification and characterization of urban heat islands (UHIs) refers to densely populated urban regions within cities where temperatures are noted to be greater than those in the surrounding or suburban areas(Pandey et al., 2014). Due to the heterogeneity of surface coverage of the land and other atmospheric elements, the standard model for Urban Heat Island (UHI) is based on LST that changes geographically. The most important variable in determining the greatest and lowest temperatures at a certain place is the LST (Ramasamy & K., 2020).

Climate change is mostly caused by global warming. Delhi's increasing temperatures are a result of urbanization, notably the creation of urban heat islands (Intergovernmental Panel on Climate Change (IPCC), 2023). It is estimated that between 2015 and 2100, over 92% of the capital's growth will take place under the best feasible emission scenario Representative Concentration Pathway (RCP) 2.6, the increase in mean temperature is predicted to be 2°C by the end of the century, while the moderate RCP 4.5 emission scenario would result in a rise of 2.9°C. Urbanization, and more specifically the creation of urban heat islands, is a factor in Delhi's increasing temperatures. Between 2015 and 2100, about 92% of the capital's growth is projected to take place. By the end of the century, the best emission scenario, Representative Concentration Pathway (RCP) 2.6, predicts a rise in mean temperature of 2°C, while the moderate RCP 4.5 emission scenario predicts a rise of 2.9°C(Intergovernmental Panel on Climate Change (IPCC), 2023). A shift in the world's climate that causes temperatures to rise over extended periods of time is referred to as global warming. Greenhouse gas emissions from power plants are the primary contributor to global warming, followed by industrial operations, transportation fuels, and agricultural practices. The availability of geospatial tools and techniques has enabled researchers to study the climate variability of New Delhi in a more comprehensive and accurate manner.

Over the last fifty years, satellite-based remote sensing has come out as among the most important technique for mapping the Earth's surface at the regional, local, and worldwide levels. A vast number of very critical applications presently rely on data from satellites. For monitoring the weather, making predictions about pollution and climate change, etc., assessments of the environment are utilized ('CERES – Clouds and the Earth's Radiant Energy System', n.d.). Land-based remote sensing from satellite significantly provide to the floods and droughts monitoring (Jeyaseelan, 2004), vegetation (Xie et al., 2008), deforestation (Gao et al., 2020), agricultural monitoring (Atzberger, 2013), urban planning (Kadhim & Bray, 2016). The efficiency of satellite data and GIS are the significant process for sub-watershed classification and natural resources conservation (Chauhan et al., 2022). Geospatial technology, such as satellite imaging, geographic information systems (GIS), and spatial interpolation methods, may analyse and show climate data spatially explicitly. Mapping of vegetation or terrain cover the regional or local scale is ideal for data with a medium spatial resolution, such as that from the LANDSAT. The Operational Land Imager (OLI) and the Thermal Infrared Sensor (TIRS) are the two sensors that LANDSAT 8 is equipped with. Eight bands in the visible, near-infrared, and shortwave infrared areas of the electromagnetic spectrum are used by OLI to gather data at a spatial resolution of 30m. An extra panchromatic band with a spatial resolution of 15m is also collected by OLI.

The study area taken in this research is New Delhi which is the capital of India and a part of the National Capital Territory of Delhi (NCT). Northern India, between latitudes of 28°24'17" and 28°53'00" North and longitudes of 76°50'24" and 77°20'37" East, is where New Delhi is situated (Figure 1). Uttar Pradesh and Haryana both share a boundary with Delhi. In the vicinity of New Delhi, the study's scope is 1,482 km^2. The Indo-Gangetic alluvial plains, the Thar Desert, and the Aravalli hill ranges all encircle New Delhi, the nation's capital, on its north and east, west, and south, respectively. The landscape is mostly flat, with the exception of a tiny, NNE-SSW sloping ridge that is regarded to represent an extension of the Aravalli hills in Rajasthan. The eastern part of the ridge on the right side of the river extends as far as Okhla in the south and disappears behind the Yamuna alluvium in the northeast.

Delhi's topography is influenced by the Yamuna River, the Aravalli Range, and the plains between them. The Delhi Ridge and its four subdivisions, the Northern, Central, South Central, and Southern, make up the longest portion of the Aravalli range. Its spurs cross the Yamuna at two locations, in the north and east. The Ridge serves as an ecological fence between the Thar Desert and the lowlands, slowing the flow of wind and dust from the desert. The natural forest that makes up this green belt moderates the warmth. The Yamuna River and the southernmost part of the Aravalli hill range are the city's two main geographical features. At an altitude of roughly 6387 metres above mean sea level, the Yamunotri glacier serves as the source of the Yamuna River. The river's whole length, from its beginning to its confluence at Allahabad, is 1376 kilometres.

The climate of study area has a subtropical climate characterized by hot summers and cool winters. The area experiences a monsoon season Indian summer monsoon (ISM) from June to September, during which it receives the maximum of its annual rainfall. The average temperature varies throughout the year, from around 14 degrees Celsius in the winter to about 46 degrees Celsius in the summer. The average annual rainfall is 714 millimetres (28.1 inches), most of which rains during the monsoons in July and August. New Delhi is also known for its high levels of air pollution, which are influenced by various factors, including emissions from vehicles and industrial activities, weather patterns,

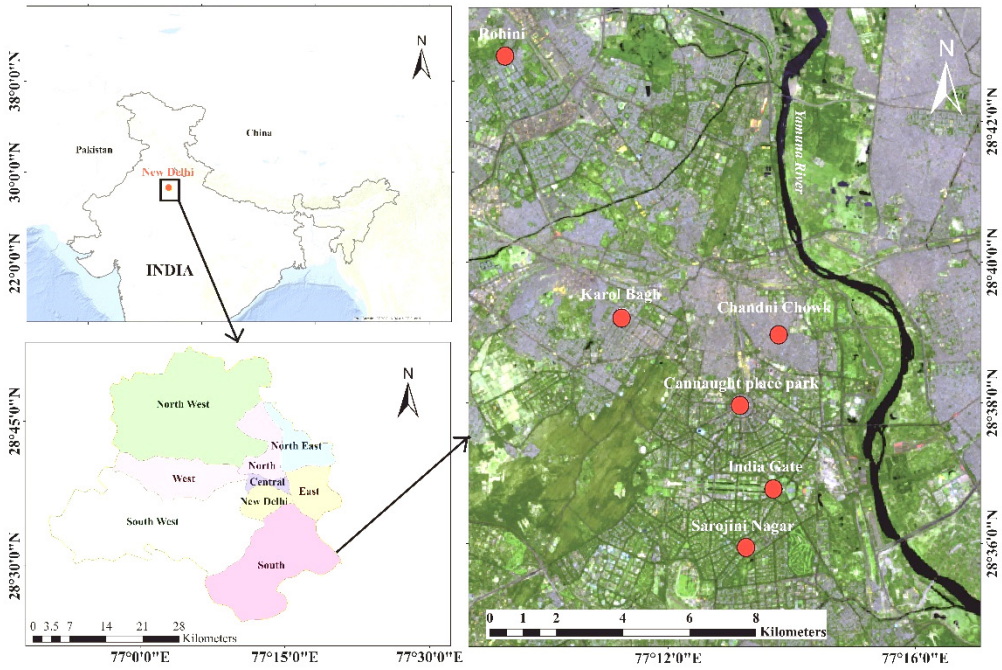

Figure 1. Location map of study area, left upper panel indicates the location of the study in India and Asia. Lower left panel describes the studied districts in New Delhi, classified FCC urban (Band combination: 7, 6, 4) in right panel describes the detail of the study area.

and geographical features. Extreme weather occurrences, fluctuation in temperature, and precipitation patterns are among the many of the effects that climate change is predicted to have on the climate.

The air quality of New Delhi has been a major concern over the past few decades. The city has been listed as one of the most polluted in the world due to excessive levels of particulate matter, nitrogen oxides, and other pollutants. These high levels of air pollution have been linked to several adverse health effects, including respiratory illnesses, cardiovascular diseases, and premature deaths. The principal cause of air pollution in New Delhi includes vehicular emissions, industrial activities, and biomass burning. New Delhi ranks 154th out of 230 cities in Mercer's 2015 annual quality-of-living ranking. In 2014, the World Health Organization ranked New Delhi as the world's most polluted city. Also was named the world's most polluted metropolis by the United States Environmental Protection Agency in 2016 and the world's most polluted capital city for the following year 2019 by IQAir.

2. Methods

The study has been carried out by both remote sensing satellite data and ground derived meteorological parameters. The remote sensing data of LANDSAT 5 and 8 at 30 m resolution has been used for the study as shown in (Table 1). One of NASA's (National Aeronautics and Space Administration) Landsat series is LANDSAT 8. The United States Geological Survey's (USGS) Earth Explorer website has access to Landsat 8 and 5 data (https://earthexplorer.usgs.gov/). Every 16 days, the LANDSAT 8 satellite captures an image of the whole planet. In the present study, bands 4 and 5 of LANDSAT 5 were used to produce NDVI of the study area. The characteristic of the dataset used in this study is demonstrated in (Table 1). The study has been carried out, using geospatial software i.e., ArcGIS 10.8 and Erdas Imagine 2014. To analysis of the LST, UHIs, and NDVI, the datasets used for the years 1993, 2000, 2010 and 2020, whereas the datasets for the years 1989, 2000, 2010 and 2020 were used to quantified the precipitation, relative humidity and wind speed in this study. Figure 3 flow chart illustrates the methods used for this investigation.

In this study, thermal bands of LANDSAT-5 & 8 were used to extract LST and to mark UHIs. IDW technique is used to carry out interpolation for the estimate the nearby point or feature such as temperature, precipitation, and wind speed at locations where the data is not available. Modelled data of precipitation, humidity and wind speed data were also collected from TerraClimate catalog Portal (http://thredds.northwestknowledge.net:8080/thredds/catalog/TERRACLIMATE_ALL/data/catalog.html), and refined with interpolation technique to estimate unknown values between known values.

Interpolation techniques

Geospatial tools from the previous three decades are used in this study. Use data from ground-based weather stations and satellite-based remote sensing to analyze variations in rainfall, temperatures, and other climate-related variables.

In this study we have employed spatial interpolation technique to estimate the climatic parameters at locations where data is not available. In order to get an estimate of rainfall based on the closest neighbouring station, (Thiessen, 1911) investigated interpolation approaches for the problem of rainfall. He employed polygons created around the positions of rainfall meters on a station network map. Several studies reported the used of the interpolation techniques in their work (Shepard, 1968). The basic idea behind interpolation is to use the available data to create a continuous surface or model of the climatic parameter being studied. Inverse Distance Weighting (IDW) method is utilized to perform interpolation. In Figure 2, the value of the unknown point is estimated as a weighted average of the known points surrounding it. The weights are calculated based on the distance between the known points

Table 1. Detail of the satellite data used in the study

Path / Row	Sensor	Acquisition Date	Spatial Resolution	Spectral Band with Wavelength (μm) (Only used band listed)
145/040	Landsat-8 (OLI)	2020/06/16	30m	Band 1 Costal (0.43–0.45) Band 2 Blue (0.45–0.51) Band 3 Green (0.53–0.59) Band 4 Red (0.63–0.67) Band 5 NIR (0.85–0.88) Band 6 SWIR-1 (1.57–1.65) Band 7 SWIR-2 (2.11–2.29) Band 8 Pan (0.50–0.68) Band 9 Cirus (1.36–1.39)
	Landsat-5 (TM)	1993/06/7 2000/05/6 2010/06/22	30m	Band 1 Blue (0.45-0.52) Band 2 Green (0.52-0.60) Band 3 Red (0.63-0.69) Band 4 Near infrared (0.76-0.90) Band 5 Mid-infrared (1.55-1.75) Band 6 Thermal infrared (10.4-12.50) Band 7 Mid-infrared (2.08-2.35)

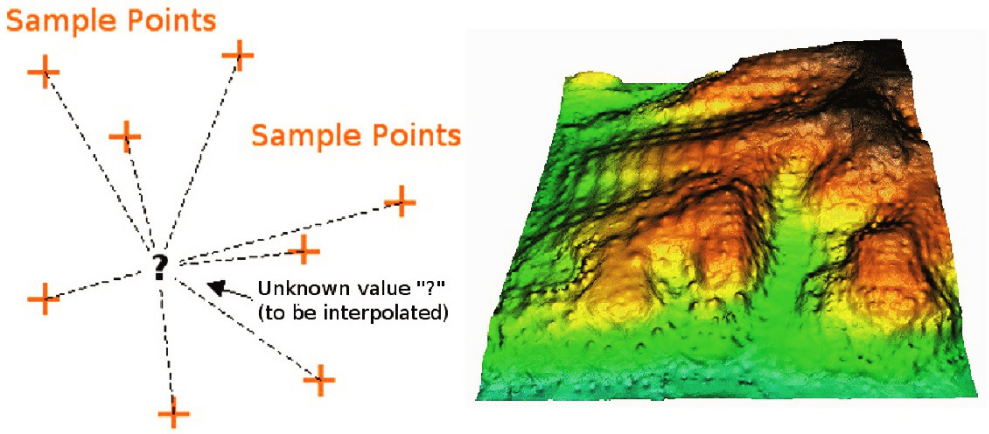

Figure 2. Inverse Distance Weighting (IDW) method of interpolation

and the unknown point, with closer points having a higher weight.

Estimation of Land Surface Temperature (LST)

Land surface temperatures (LST) were estimated using LANDSAT 5 and 8 satellite data for the year 1993, 2000, 2010 and 2020. LST is calculated as given formulas:

Step 1: Convert DN value to radiance using the equation 1:

$$L(\lambda) = \frac{L_{max} - L_{min}}{255} * DN + L_{min} - Oi = 0.0003342 * \text{Band10} + 0.1 - 0.29 \quad (1)$$

where $L(\lambda)$ is the radiance in (W/m2/sr/mm), L_{max} is the maximum value of spectral radiance, L_{min} is the minimum value of spectral radiance in (W/ m²*sr*μm), and 255 is the maximum calibrated digital number value in image, and DN is the digital number.

Step 2: The brightness temperature was calculated using the following equation 2:

$$T = \frac{K_2}{\ln\left(\frac{K_1}{L_\lambda} + 1\right)} - 273.1 \quad (2)$$

where T is the radiance temperature in degrees Celsius, K_1 and K_2 are thermal calibration constant values, and L_λ is the top of atmosphere radiance of the sensor in (W/m²/sr/μm).

Step 3: Calculate NDVI.

$$NDVI = NIR - R / NIR + R \quad (3)$$

Where, NIR is Near Infrared Band and R is Red Band.

Step 4: Calculate proportion of vegetation (P_v).

$$P_v = \left(\frac{NDVI - NDVI_{min}}{NDVI_{max} - NDVI_{min}}\right)^2 \quad (4)$$

where, P_v is the proportion of vegetation, $NDVI$ is the normalized difference vegetation index.

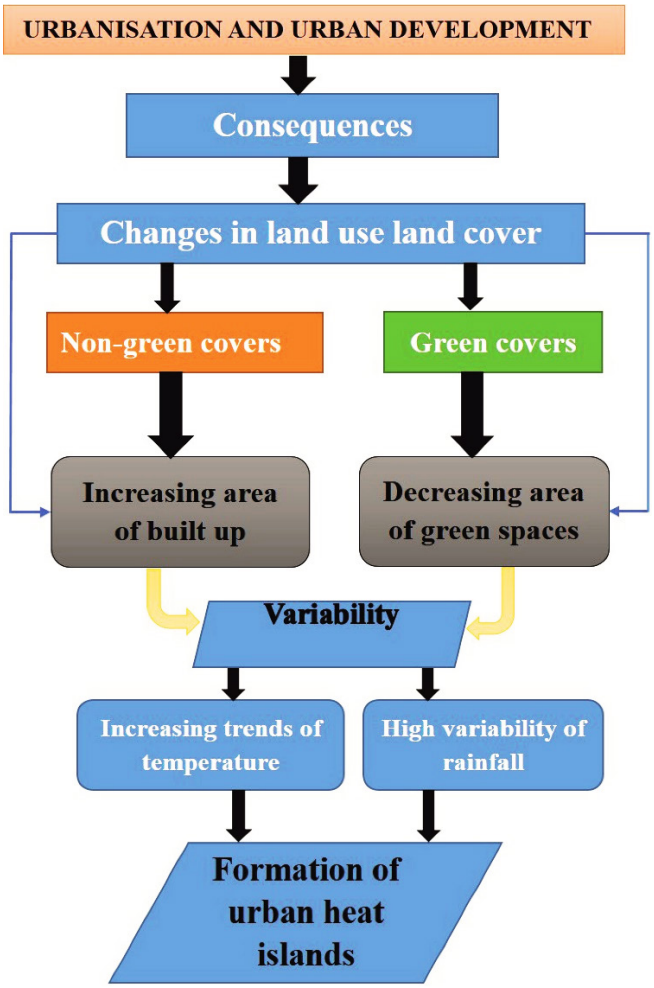

Figure 3. Flow diagram of methodology adopted in the study

Step 5: Calculate emissivity.

$$\varepsilon = \varepsilon_s\lambda + (\varepsilon_v\lambda - \varepsilon_s\lambda)P_v \quad (5)$$

where ε is the calculated emissivity, ε_v and ε_s represents soil and vegetation emissivity, respectively, and P_v is the fraction of vegetative cover.

Step 6: After calculation of the land surface emissivity, the following equation was applied to estimate the LST as given in equation 6:

$$LST = (T / (1 + (0.00115 * T / 1.4388) * ln(\varepsilon))) \quad (6)$$

For LANDSAT 5:
Step1:

$$L(\lambda) = \left(\frac{LMAX_\lambda - LMIN_\lambda}{QCALMAX - QCALMIN}\right) * (QCAL - QCALMIN) + LMIN_\lambda \quad (7)$$

Where $L(\lambda)$ is spectral radiance, $QCAL$ is quantised calibrated pixel value in DN, LMAXλ is spectral radiance scaled to $QCALMAX$ in Watts/m^2*sr*µm), $LMIN\lambda$ is spectral radiance scaled to $QCALMIN$ in Watts/ m^2*sr*µm, $QCALMIN$ is minimum quantised calibrated pixel value in DN, $QCALMAX$ is maximum quantised calibrated pixel value in DN.

Step 2: Convert Radiance to Brightness temperature.

$$T = \frac{K_2}{\ln\left(\frac{K_1}{L_\lambda} + 1\right)} - 273.1 \quad (8)$$

Where, K1 and K2 are calibration constant1 and constant2, Lλ is spectral radiance in Watts/m^2*sr*µm).

Urban heat islands (UHI)

T = Surface temperature (LST)
µ = Average surface temperature value
α = Standard deviation of surface temperature

$$UHI = Tmean - (\mu + 0.5\,\alpha) \quad (9)$$

UHI = Urban Heat Island
$Tmean$ = Land Surface Temperature (°C)
μ = LST mean value (°C)
α = LST standard deviation value (°C)

Positive temperature difference value indicates that the area is experiencing UHI. If it is negative, then UHI phenomenon does not occur in the area.

Normalised Difference Vegetation index (NDVI)

Normalized Difference Vegetation Index (NDVI) was calculated from satellite data using the equation 10.

$$NDVI = NIR - RED / NIR + RED \quad (10)$$

Where, NIR is Near Infrared Band (Band 4 of Landsat 5 data); R is Red Band (Band 3 of Landsat 5 data).

Land Use Land Cover (LULC) analysis

The multi-spectral LANDSAT series satellite data (Table 1), which was retrieved from the USGS Earth Explorer portal, was used to create the LULC maps for the current investigation. The false color composite (FCC) was created using the downloaded data for the years 1989, 2000, 2010, and 2020. Through the use of the K-means unsupervised classification algorithm, LULC mapping was completed. The Bhuvan-Indian Geo-Platform of ISRO was used to determine the LULC classes in the research area.

3. Results and Discussion

Land Surface Temperature (LST)

The study area has experienced significant temperature variations over the past few decades. The temperature varies from 46 °C (115 °F) in the summer to around 0 °C (32 °F) in the winter. Studies have shown that there has been a clear warming trend in the city, with temperatures rising by an average of 0.5 to 1 degree Celsius over the past few decades (2018 - Global Warming of 1.5°C). The rate of warming has been higher during the winter months, with an increase of around 1 to 1.5 degrees Celsius observed since the 1980s (Rajput et al., 2023). The warming trend in New Delhi is believed to be primarily driven by human activities, including increasing greenhouse gas emissions and urbanization. This increase in temperature has several implications, including an increased risk of heatwaves and associated health impacts, reduced agricultural productivity, and changes in the timing and intensity of the monsoon season. To understand the climatic variability and changing weather pattern, decadal climatic parameters maps were prepared using satellite and available meteorological data.

The analysis of decadal (1993–2020) changes shows that LST has increased from 45.93°C to 52.83°C with standard deviation (SD±6.35). Interestingly, LST drop down 35.86°C in the year 2000, and the years 2010 and 2020 has achieved the LST trend 41.31°C and 52.83°C in increasing trend. Minimum LST from 1993 to 2020 estimated to be 25.40°C to 26.09°C (SD±6.35), which is also shows the increasing trend except the year 2000 as 21.94°C. In the past three decades except for the year 2000 where temperature drops by approximately 10 °C. M For the year 2000 temperature drops by approximately 10 °C but it increases in the year 2010 when temperature reaches 40.311 °C. (Figure 4 and Table 2).

Urban Heat Island (UHIs)

Urban heat islands are characterized as metropolitan regions that are much warmer than the nearby rural areas as a result of human activity (Takebayashi et al., 2020). Previous research indicates that more than 40% of metropolitan land areas are covered with asphalt pavement, which substantially consider for the urban heat island phenomena in most cities. This caused the yearly growth to coincide with the acceleration of urbanization. The creation of innovative technology to lessen the urban heat island effect is crucial in the context of this global warning.

Public health is significantly at danger from urban heat stress. As with other environmental stressors, heat exposure may be asymmetrically distributed between income levels, according to prior case studies of specific cities (Hsu et al., 2021). In our study maximum UHIs values in 1993 and 2020 with (SD±0.18) were reported 3.36 and 5.12 respectively

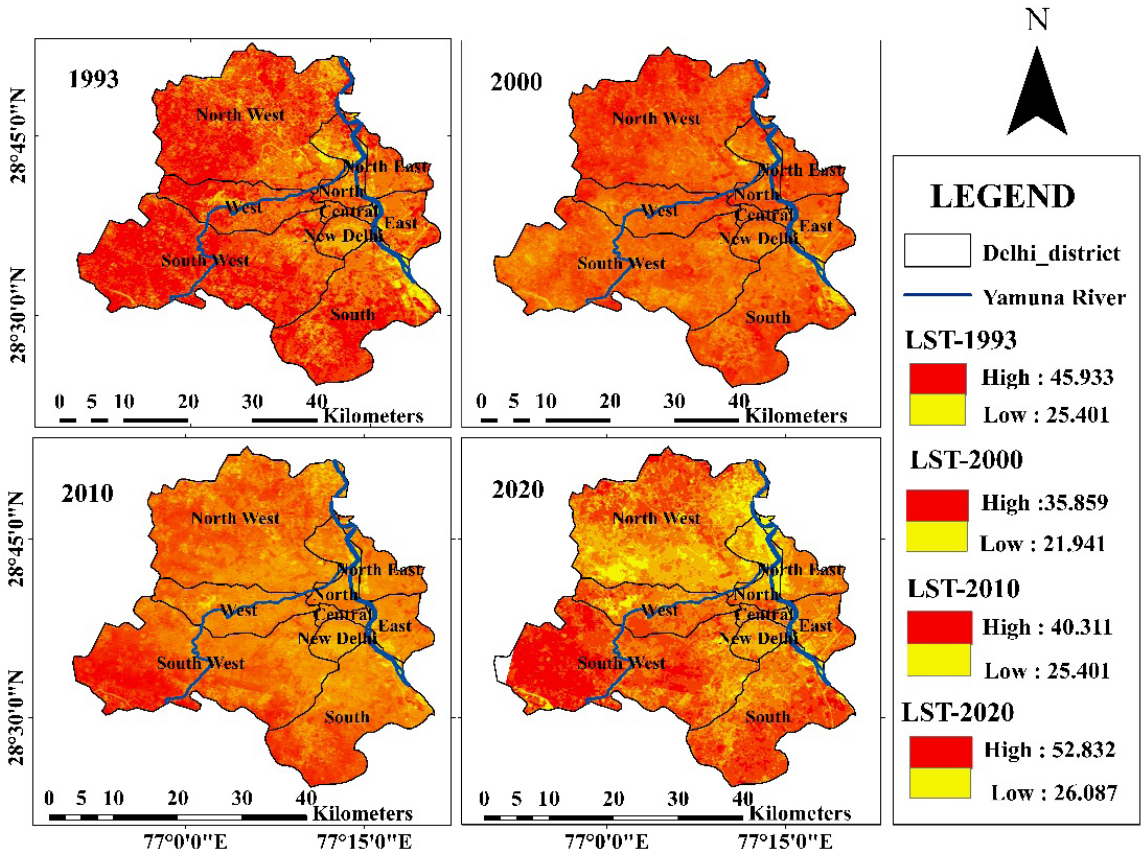

Figure 4. Decadal (1993-2020) map of Land Surface Temperature (LST)

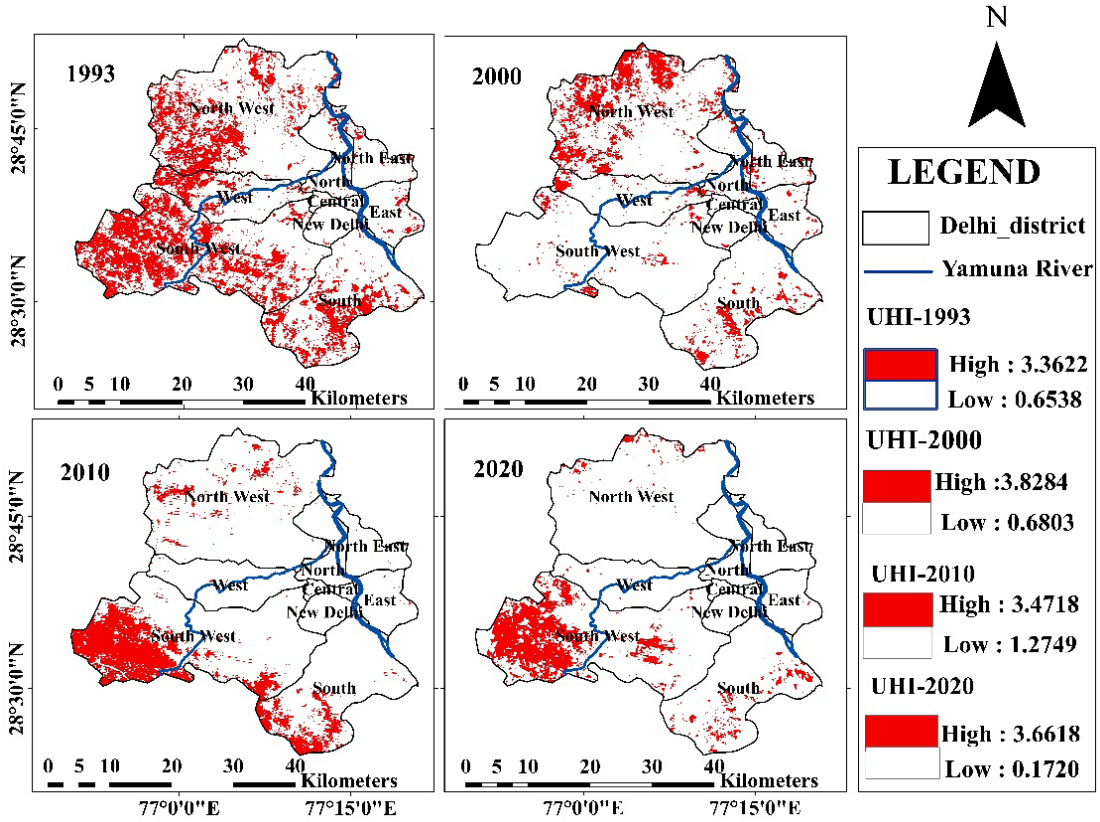

Figure 5. Decadal (1993-2020) UHIs map of the study area

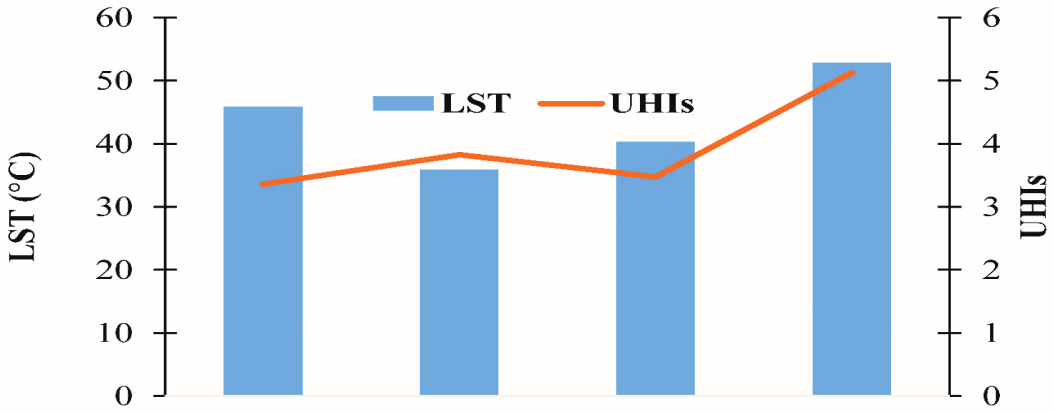

Figure 6. Correlation of LST and UHIs, which indicates the positive relationship between LST and UHIs

in high class. In the low class with (SD±0.39) were reported maximum in the year 2010 as 1.28, whereas the minimum estimated to be 0.65 in the year 1993. The decadal UHIs values from 1993 to 2020 shows an increasing trend, which is the evidence of the climate variability in the study area (Table 2 and Figure 5). The Figure 6 shows that the UHIs in increased trend if the LST enrich, which indicates that temperature is the most common factor to increases the UHIs and contributes to the global warming and climate change.

Precipitation

Rainfall is an important climatic parameter that influences several aspects of weather, including temperature, humidity, and agricultural productivity. In the study area, rainfall patterns have varied over the past few decades. Studies have shown that the city of New Delhi has experienced an overall decreasing pattern in rainfall, particularly during the monsoon season, which is the primary source of rainfall in the region (Rajput et al., 2023). According to the India Meteorological Department (IMD), an average monsoon rainfall in New Delhi has decreased from around 67 cm in the year 1970s to around 50 cm in recent years. This trend of rainfall is believed to be primarily driven by changing of climate, including shifts in the monsoon season and changes in atmospheric circulation patterns

The decrease in rainfall has several implications, including reduced agricultural productivity, increased risk of water scarcity, increased vulnerability to droughts and other climate-related hazards. The estimated precipitation for the present study from the years 1989 to 2020, maximum precipitation was estimated to be 70.07cm in the year 2020 and minimum 44.22cm in the year 2000 with (SD±9.84) for the entire study period. The years 1989 and 2010 has quantified the precipitation values 65.80cm and 62.23cm respectively.

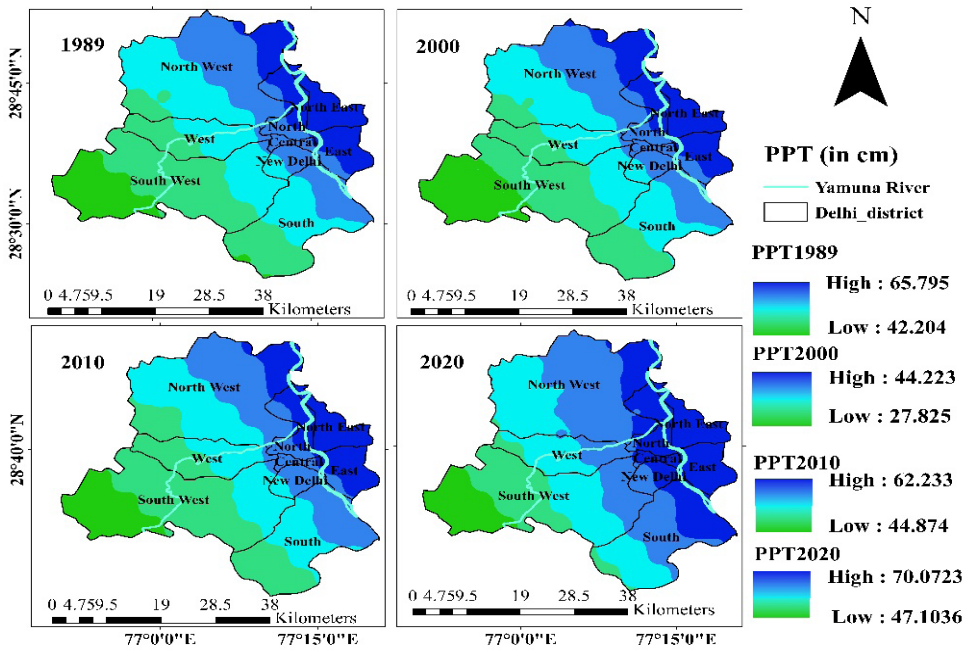

Figure 7. Classified precipitation map of the study area, shows the decadal precipitation variability in the study area

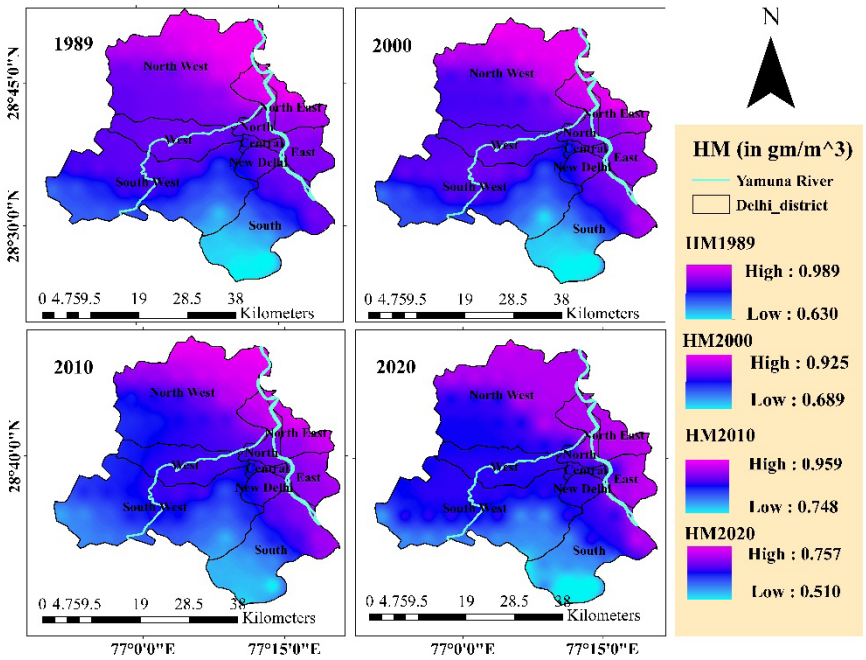

Figure 8. Classified humidity map of the study area shows the decadal humidity in the study area

The map shows the low-class values for the precipitation, highest in the year 2020 as 47.10cm and lowest as 27.83cm in the year 2000, the detail the precipitation can be seen in the (Table 2 and Figure 7).

Relative Humidity (RH)

Relative humidity is an important meteorological parameter that influences the Earth's climate and weather patterns, which is also the indicating outcome parameter of the temperature. It relates to how much water vapor is in the air and is sometimes represented as a percentage of how much moisture may safely be retained at a particular temperature. An average relative humidity during the summer months has increased from around 40% in the 1970s to over 50% in recent years. Changes in humidity can have a significant impact moisture source, including the frequency and intensity of rainfall, as well as the occurrence of maximal weather events such as heat waves, droughts and extreme rainfall events.

High humidity is mainly found in areas adjacent to Yamuna River like North West, North East and East Delhi while low humidity is present in South Delhi area having high altitude and barren land. From 1989-2020 humidity changes from 0.99 g/cm^3 to 0.76 g/cm^3 with (SD±0.09). In the year 2000 humidity decreases to 0.93 g/cm^3 which is due to decrease in rainfall in the same year. There is slight increase in humidity 0.96 g/cm^3 in 2010 but there is gradual decrease in the year 2020 when humidity value reaches to 0.76 g/cm^3 as the temperature reaches to 52.83°C. The low to high values map of the humidity are presented in the (Table 2 and Figure 8).

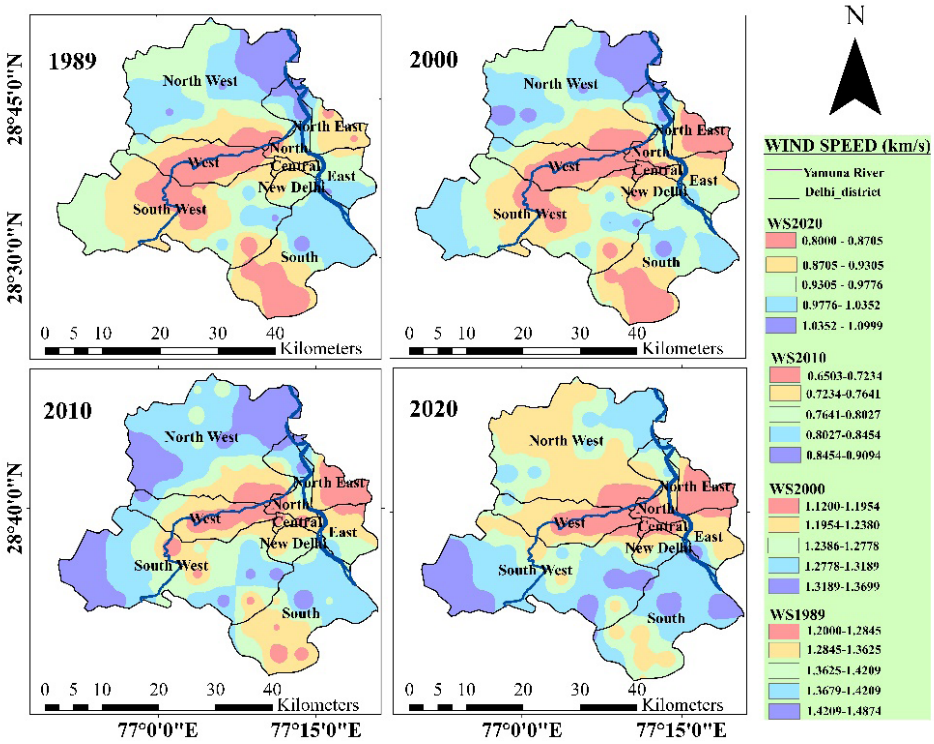

Figure 9. Classified wind speed map of the study area hows the decadal wind speed in the study area

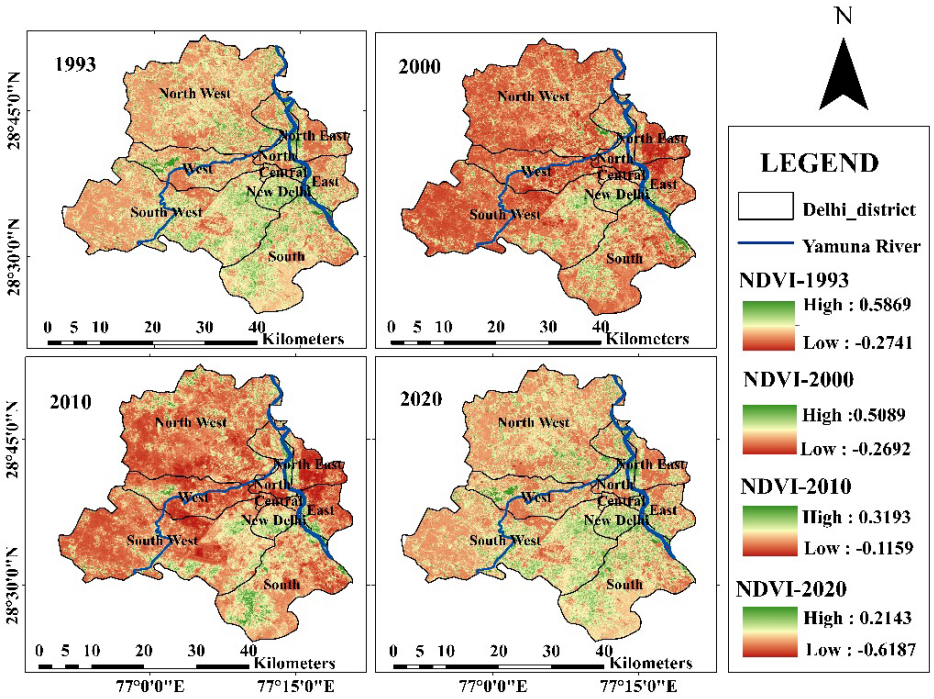

Figure 10. Shows the decadal (1993-2020) Normalized Difference Vegetation Index in the study area

Wind Speed (WS)

Wind speed is an important climatic parameter that influences several aspects of weather, including temperature, humidity, and precipitation. In New Delhi, wind speed has varied over the past few decades, with some studies indicating a declining trend. According to data from the India Meteorological Department, the average wind speed during the winter months has decreased from around 10 km/h in the 1970s to around 6 km/h in recent years (Krishan et al., 2019). Similarly, the average wind speed during the summer months has decreased from around 8 km/h in the 1970s to around 5 km/h in recent years. The decrease in wind speed has several implications, including an increase in air pollution levels and a higher risk of heat-related illnesses due to reduced air movement.

In the studied period, three decades wind speed slightly decreases from 1.48 km/s to 1.03 km/s (SD±0.23). In high class maximum wind speed was calculated to be 1.48 km/s in the year 1989, whereas the minimum 0.90 km/s noted in the year 2010. Years 2010 and 2020 the wind speed was observed 1.31 km/s and 10.3 km/s respectively. The wind speed map and its class from low to high decadal has presented in the (Figure 9 and Table 2).

Normalised Difference Vegetation Index (NDVI)

NDVI values ranges from -1 to +1. Negative NDVI values shows presence of water bodies while NDVI values close to +1 indicates dense green vegetation. On the other hand, values close to 0 indicates built up area. There is significant decrease in NDVI value 0.58-0.21 (SD±0.15) from 1993-2010 which is attributed to decrease in rainfall amount and increase in built up area which reduces green cover.

The Maximum NDVI value estimated to be 0.59 in the year 1993 and minimum 0.21 in the year 2020, which indicated that the green area of the study region is converting with settlement and built-up area. The years 2000 and 2010 have quantified the NDVI values as 0.51 and 0.31 respectively, these two decades has shown the NDVI values in decreasing trend. The Low to high class NDVI values are presented in (Figure 10 and Table 2).

Land use and Land Cover (LULC)

Local urbanisation and large-scale climatic processes both have an impact on warming trends in cities (Liu et al., 2022). LULC classification is the most important analysis for the estimated the UHIs and NDVI and understand the climate change pattern of the particular region. In LULC maps features were classified into different classes such as agricultural land, built up area, barren and scrub land, water bodies and forest area. Area for each feature class has been quantified as shown in (Figure 11 and 12). In the past three decades there has been rapid expansion in settlement area and agriculture land (Figure 11). In the year 1989 maximum area 715.29 km^2 (48.27%) was covered with agriculture land and minimum 32.0 km^2 (2.16%) of water bodies. The area covered by the barren & scrub, built0up land and forest was 209.56 km^2 (14.14%), 327.0 km^2 (22.06%) and 198.15 km^2 (13.37%) respectively. The maximum area in 1989 (48.27%) was covered by the agriculture, whereas in the year 2020 the area was decreased as 402.21 km^2 (27.14%) with ~ 1.8 times lower from 1989 to 2020. The other decadal decreasing trend can be seen in the (Figure 11 and 12). The decadal changes can also be seen from the year 1989 to 2020, in LULC categories i.e., barren & scrub land and water bodies, as ~ 3.3 and ~1.2 times respectively in decreasing trend. The Barren land and forest area was dramatically changes with built-up land, as the area was quantified of built-up land in the year 1989 as 327.0 km^2 (22.06%) and the decadal increasing trend in all studied years reached at 794.68 km^2 (53.62%) in 2020, which indicates the rapidly changes from green area to built-up land, which

Table 2. Quantified values for various climatological parameters

Year	Value		Parameters
	Max	Min	
1993	45.93	25.40	
2000	35.86	21.94	
2010	40.31	25.40	LST (°C)
2020	52.83	26.09	
SD	6.35	1.62	
1993	3.36	0.65	
2000	3.83	0.68	
2010	3.47	1.28	UHI
2020	5.12	1.27	
SD	0.18	0.39	
1989	65.80	42.20	
2000	44.22	27.83	
2010	62.23	44.87	Precipitation (cm)
2020	70.07	47.10	
SD	9.84	7.52	
1989	0.99	0.63	
2000	0.93	0.69	
2010	0.96	0.75	Humidity (gm/m^3)
2020	0.76	0.51	
SD	0.09	0.09	
1989	1.48	1.28	
2000	1.31	1.19	
2010	0.90	0.65	Wind speed (km/s)
2020	1.03	0.87	
SD	0.23	0.25	
1993	0.59	-0.27	
2000	0.51	-0.27	
2010	0.32	-0.12	NDVI
2020	0.21	-0.62	
SD	0.15	0.18	

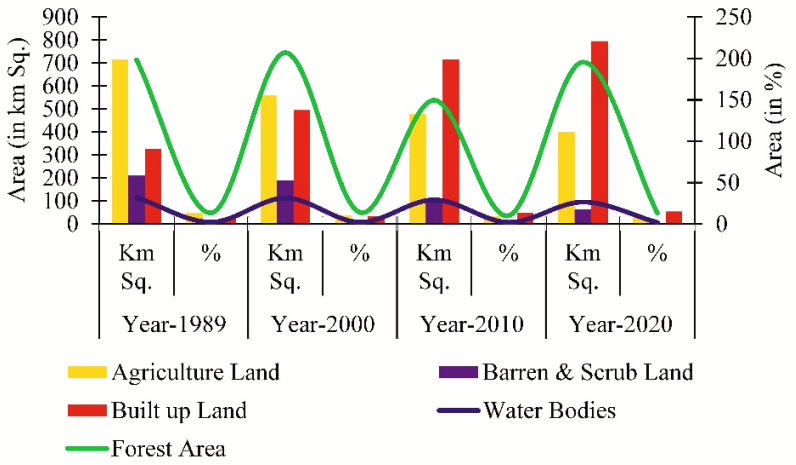

Figure 11. Decadal LULC changes, graph shows the area in sq. km and percentage of each land used and land cover category

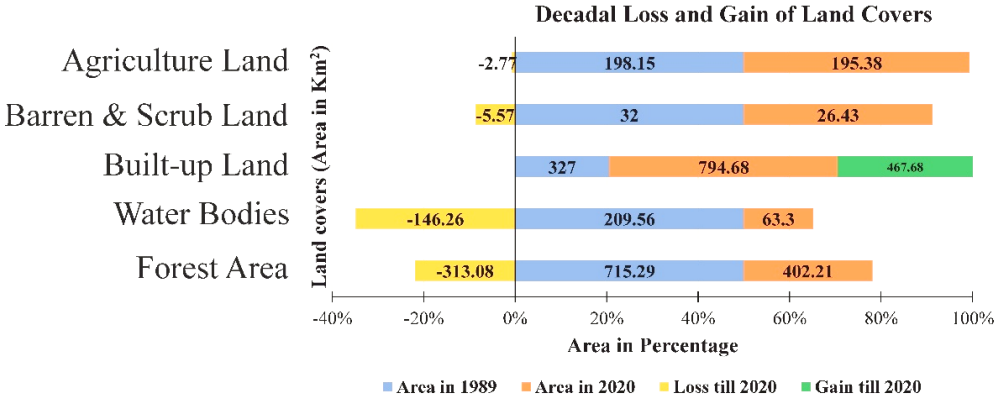

Figure 12. Decadal (1989-2020) change of loss and gain scenario of LULC categories, which indicates the drastic changes from green cover area to built-up land, in the study area

Table 3. Classified LULC Features and its estimated areal coverage in the study area

Year	1989		2000		2010		2020	
LULC Category	Km²	%	Km²	%	Km²	%	Km²	%
Agriculture Land	715.29	48.27	558.28	37.67	477.31	32.21	402.21	27.14
Barren & Scrub Land	209.56	14.14	190.24	12.84	111.12	7.50	63.3	4.27
Built up Land	327.00	22.06	495.36	33.43	715.11	48.25	794.68	53.62
Water Bodies	32.00	2.16	31.29	2.11	29.08	1.96	26.43	1.78
Forest Area	198.15	13.37	206.83	13.96	149.38	10.08	195.38	13.18
Total	*1482.00*	*100.00*	*1482.00*	*100.00*	*1482.00*	*100.00*	*1482.00*	*100.00*
Min	*32.00*	*2.16*	*31.29*	*2.11*	*29.08*	*1.96*	*26.43*	*1.78*
Max	*715.29*	*48.27*	*558.28*	*37.67*	*715.11*	*48.25*	*794.68*	*53.62*

promotes the UHIs as increased. Consequently, rapid decrease in the green cover from 48.27% to 27.14% in agricultural land and 14.14% to 4.27% in barren and scrub. The detail decadal changes in all LULC categories are presented in (Table 3 and Figure 11). The Figure 12 shows that an area change in LULC from 1989 to 2020 and decadal loss and gain of land cover form entire study period. The LULC loss and gain analysis was carried out, which revealed that the urban and built-up area has rapidly expanded as 467.68 km², whereas agricultural land, barren & scrubs, water bodies and forest area shows in decreasing trend as 2.77 km², 5.57 km², 146.26 km² and 313.08 km² respectively.

Correlation of LST with NDVI

In the study, correlation between LST and NDVI is shown in Figure 13. LST and NDVI were shown to be negatively correlated. correlation results stated that these relationships, higher NDVI leads to lower LST, and lower NDVI leads to higher LST. Study carried out by (Jabbar et al. 2022) in Pakistan and proved that, 5°C decrease in LST corresponds to the increase of NDVI by 0.5. From our study resultant that it is clear that LST decreases with increasing NDVI. Similarly, LST increases with decreasing NDVI. This correlation indicates that urban green cover may contribute to LST decrease and can help to maintain thermal uniformity in cities.

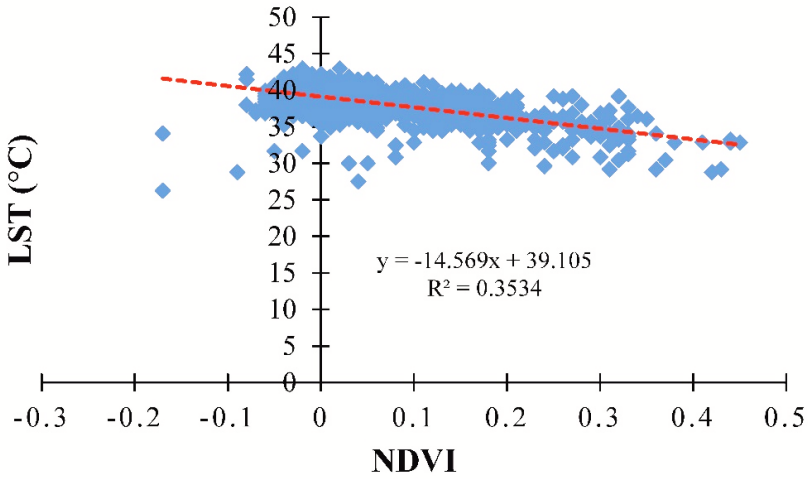

Figure 13. Correlation between Land surface Temperature (LST) and Normalized Difference Vegetation Index (NDVI) in the study area

Discussion

Both the air and land surface temperatures are affected by altering in land use and cover. (Jabbar & Yusoff, 2022). Due to the LULC Changes, LST has increased drastically in last three decades and they also affect the air temperature. Outcome of this study narrate that increasing of LST and UHIs is caused by the conversion of the green area by the built-up land and changes in the land surface structure, energy use, and an increase in impermeable surfaces like buildings and concrete pavements. Previously, study carried by (Jabbar et al., 2013) has found that, the LST and UHIs shows an increasing trend due to the loss of urban green area and rapid growth of built-up land. The results show the LST values are higher in contrast to the rural equivalent. Based on the calculated LST, the UHIs have been derived for the year 2000, which is comparatively less, UHIs are formed as there is significant decrease in LST for this decade. In comparison to suburban or rural regions, Delhi's urban areas with high urban density have lower LST's. Concrete structures with some nearby plants can create local shade in densely populated regions, lowering the surface temperatures. Contrarily, Delhi's rural parts are dry, fallow grounds without any vegetation or shade, which trap heat from shortwave radiation and raise LST according to data from the LANDSAT 8 satellite." By comparing the amount of red and NIR light that the plant absorbs and reflects, the NDVI measures the amount of vegetation. For negative values of NDVI it is more likely that it is water while NDVI value close to +1 shows high possibility that it is green cover. But NDVI values close to zero means urbanised area. In the past three decades there has been increase in LST and decrease in NDVI values. According to the correlation, the relationship between NDVI and LST are inversely associated, or adversely connected, with one another. If LST increases the NDVI value decreases. The decrease in NDVI value is attributed to increase in built up area and decrease in green cover as shown in the study. The increase in UHIs effect is a consequence of constantly growing population which simultaneously increases urbanisation. It can be controlled by proper planning of urban places with compulsory garden and by mandatory planting trees in the middle and both sides of roads and on rooftops.

4. Conclusion

The studied results show that, the capital of the i.e., Over the past few decades, there has been a noticeable rise in temperature in New Delhi. The study reveals that LST have significantly increased from 45.934 °C to 52.832 °C. The primary causes of climate change are the significant increase in urbanization and the decline in natural cover. The LULC analysis shows that the built-up area has increased drastically, from 22.06% to 53.62% from 1989 to 2020 and agricultural land have decreased from 48.27% to 27.14%. Among the most important elements contributing to the fast urban expansion around cities is the Urban Heat Island (UHI) phenomenon. The wind speed is low in settlement areas because of concrete structures that blocks blowing air while it is high in open agricultural or crop land. The drastic percent change of the agriculture land in the year 1989 as 48.27% to 27.14% in the year 2020. The green cover area was rapidly altered in the built-up land from 22.06% to 53.62% in the years 1989 to 2020 respectively. The barren and scrub land were converted in the built-up land, as significant changes from 1989-2020 as 14.14% to 4.27% respectively. The impacts of these changes are visible in various sectors, including agriculture, air quality, and human health. Therefore, a present study clearly shows the vast climate variability and rapidly increasing pattern in LST and UHIs of New Delhi, this climate change impact would not be limited to the study area and surrounding regions, whereas the indicates the drastic climate change in the Himalayan regions also. The rapid changes found LULC trend is extremely sensitive for the environment and ecological structure of the study area. The outcomes of this research will provide insights into the spatiotemporal patterns of climate variability in New Delhi and the potential impacts on various sectors such as agriculture, water resources, and public health. Further this invitation would be very significant pathway to understand the climate change variability and impact of the climate change. Results would also be fruitful for the future society as urban planners, researchers and policy makers for the future development and planning.

Acknowledgement

First author is thankful to Dean, School of Planning and Architecture for her time-to-time guidance and suggestions. Corresponding author expresses sincere thanks to the science and Engineering Research Board (SERB), DST, New Delhi, India for the financial support (SIR/2022/000972), and also grateful to the Director Wadia Institute of Himalayan Geology, Dehradun for logistic support.

References

2018 — Global Warming of 1.5 °C. (n.d.). Retrieved from https://www.ipcc.ch/sr15/2018/

Atzberger, C. (2013). Advances in Remote Sensing of Agriculture: Context Description, Existing Operational Monitoring Systems and Major Information Needs. *Remote Sensing*, *5*(2), 949–981. doi:10.3390/rs5020949

CERES – Clouds and the Earth's Radiant Energy System. (n.d.). Retrieved 2 May 2025, from https://ceres.larc.nasa.gov/

Chauhan, P., Darshan, M., Kalachand, S., Ram L., R., Sudhir Kumar, S., & and Singh, D. (2022). Assessing the vulnerability of watersheds to environmental degradation in the lesser Himalayan region using satellite data and a series of models. *Geocarto International*, *37*(27), 18372–18399. doi:10.1080/10106049.2022.2142958

Chauhan, P., Singh, N., Chauniyal, D. D., Ahluwalia, R. S., & Singhal, M. (2017). Differential behaviour of a Lesser Himalayan watershed in extreme rainfall regimes. *Journal of Earth System Science*, *126*(2), 22. doi:10.1007/s12040-017-0796-0

Gao, Y., Skutsch, M., Paneque-Gálvez, J., & Ghilardi, A. (2020). Remote sensing of forest degradation: a review. *Environmental Research Letters*, *15*(10), 103001. doi:10.1088/1748-9326/abaad7

Gašparović, M., & and Singh, S. K. (2023). Urban surface water bodies mapping using the automatic k-means based approach and sentinel-2 imagery. *Geocarto International*, *38*(1), 2148757. doi:10.1080/10106049.2022.2148757

Hsu, A., Sheriff, G., Chakraborty, T., & Manya, D. (2021). Disproportionate exposure to urban heat island intensity across major US cities. *Nature Communications*, *12*(1), 2721. doi:10.1038/s41467-021-22799-5

IMD | Environmental Monitoring Services. (n.d.). Retrieved 2 May 2025, from https://mausam.imd.gov.in/imd_latest/contents/environmental-monitoring-services.php

Intergovernmental Panel on Climate Change (IPCC). (2023). Climate Change 2021 – The Physical Science Basis. *Climate Change 2021 – The Physical Science Basis*. doi:10.1017/9781009157896

Jabbar, M., & Yusoff, M. (2022). Assessing The Spatiotemporal Urban Green Cover Changes and Their Impact on Land Surface Temperature and Urban Heat Island in Lahore (Pakistan). *GEOGRAPHY, ENVIRONMENT, SUSTAINABILITY*, *15*, 130–140. doi:10.24057/2071-9388-2021-005

Jeyaseelan, A. (2004). Droughts & Floods Assessment and Monitoring using Remote sensing and GIS. In *Satellite Remote Sensing and GIS Applications in Agricultural Meteorology*.

Kadhim, N., Mourshed, M., & Bray, M. (2016). Advances in remote sensing applications for urban sustainability. *Euro-Mediterranean Journal for Environmental Integration*, *1*(1), 7. doi:10.1007/s41207-016-0007-4

Krishan, M., Jha, S., Das, J., Singh, A., Goyal, M. K., & Sekar, C. (2019). Air quality modelling using long short-term memory (LSTM) over NCT-Delhi, India. *Air Quality, Atmosphere & Health*, *12*(8), 899–908. doi:10.1007/s11869-019-00696-7

Li, Z.-L., Wu, H., Duan, S.-B., Zhao, W., Ren, H., Liu, X., … Zhou, C. (2023). Satellite Remote Sensing of Global Land Surface Temperature: Definition, Methods, Products, and Applications. *Reviews of Geophysics*, *61*(1), e2022RG000777. doi:https://doi.org/10.1029/2022RG000777

Liu, Z., Zhan, W., Bechtel, B., Voogt, J., Lai, J., Chakraborty, T., … Lee, X. (2022). Surface warming in global cities is substantially more rapid than in rural background areas. *Communications Earth & Environment*, *3*(1), 219. doi:10.1038/s43247-022-00539-x

M, P. B., & Suresh Babu, S. (2018). Estimation of Land Surface Temperature using LANDSAT 8 Data. *International Journal of Advance Research*. Retrieved from www.IJARIIT.com

Oke, T. (1982). The energetic basis of urban heat island. *Quarterly Journal of the Royal Meteorological Society*, *108*, 1–24. doi:10.1002/qj.49710845502

O'Malley, C., Piroozfar, P., Farr, E. R. P., & Pomponi, F. (2015). Urban Heat Island (UHI) mitigating strategies: A case-based comparative analysis. *Sustainable Cities and Society*, *19*, 222–235. doi:https://doi.org/10.1016/j.scs.2015.05.009

Pandey, A. K., Singh, S., Berwal, S., Kumar, D., Pandey, P., Prakash, A., … Kumar, K. (2014). Spatio – temporal variations of urban heat island over Delhi. *Urban Climate*, *10*, 119–133. doi:https://doi.org/10.1016/j.uclim.2014.10.005

Pramanik, S., & Punia, M. (2020). Land use/land cover change and surface urban heat island intensity: source–sink landscape-based study in Delhi, India. *Environment, Development and Sustainability*, *22*(8), 7331–7356. doi:10.1007/s10668-019-00515-0

Raja, P., Singh, N., Srinivas, C. V, Singhal, M., Chauhan, P., Singh, M., & Sinha, N. K. (2018). Analyzing energy–water exchange dynamics in the Thar desert. *Climate Dynamics*, *50*(9), 3281–3300. doi:10.1007/s00382-017-3804-9

Rajput, J., Sena, D., Singh, D. K., Mani, I., & IMD, M. (2023). Trend assessment of rainfall, temperature and relative humidity using non-parametric tests in the national capital region, Delhi, *74*, 593–606.

Ramasamy, R., & K., E. (2020). Impact of urbanisation on formation of urban heat island in Tirupur region using geospatial technique. *Indian Journal of Geo-Marine Sciences*, *49*, 1593–1598.

Rastogi, T., Singh, J., Singh, N., Chauhan, P., Yadav, R. R., & Pandey, B. (2023). Temperature variability over Dokriani glacier region, Western Himalaya, India. *Quaternary International*, *664*, 33–41. doi:https://doi.org/10.1016/j.quaint.2023.05.013

Shepard, D. (1968). A two-dimensional interpolation function for irregularly-spaced data. *Proceedings of the 1968 23rd ACM National Conference, ACM 1968*, 517–524. doi:10.1145/800186.810616

Singh, D., Vardhan, M., Sahu, R., Chatterjee, D., Chauhan, P., & Liu, S. (2023). Machine-learning- and deep-learning-based streamflow prediction in a hilly catchment for future scenarios using CMIP6 GCM data. *Hydrology and Earth System Sciences*, *27*(5), 1047–1075. doi:10.5194/HESS-27-1047-2023,

Singh, N., Shekhar, M., Parida, B. R., Gupta, A. K., Sain, K., Rai, S. K., … Montagnani, L. (2022). Tree-Ring Isotopic Records Suggest Seasonal Importance of Moisture Dynamics Over Glacial Valleys of the Central Himalaya. *Frontiers in Earth Science*, *10*, 868357. doi:10.3389/FEART.2022.868357/ENDNOTE

Singh, N., Singh, J., Gupta, A. K., Bräuning, A., Dimri, A. P., Ramanathan, A. L., … Raja, P. (2021). Climate-driven acceleration in forest evapotranspiration fuelling extreme rainfall events in the Himalaya. *Environmental Research Letters*, *16*(8), 084042. doi:10.1088/1748-9326/ac14ed

Singh, S., Mall, R. K., & Singh, N. (2021). Changing spatio-temporal trends of heat wave and severe heat wave events over India: An emerging health hazard. *International Journal of Climatology*, *41*(S1), E1831–E1845. doi:https://doi.org/10.1002/joc.6814

Takebayashi, H., Misaka, I., & Akagawa, H. (2020). Chapter 2 - Adaptation measures and their performance. In H. Takebayashi & M. Moriyama (Eds.), *Adaptation Measures for Urban Heat Islands* (pp. 9–37). Academic Press. doi:https://doi.org/10.1016/B978-0-12-817624-5.00002-6

Thiessen, A. H. (1911). Precipitation averages for large areas. *Monthly Weather Review*, *39*(7), 1082–1089. doi:https://doi.org/10.1175/1520-0493(1911)39<1082b:PAFLA>2.0.CO;2

Wu, G. X., Liu, Y., Zhu, X., Li, W., Ren, R., Duan, A., & Liang, X. (2009). Multi-scale forcing and the formation of subtropical desert and monsoon. *Ann. Geophys.*, *27*(9), 3631–3644. doi:10.5194/angeo-27-3631-2009

Xie, Y., Sha, Z., & Yu, M. (2008). Remote sensing imagery in vegetation mapping: a review. *Journal of Plant Ecology*, *1*(1), 9–23. doi:10.1093/jpe/rtm005

Yang, Y.-J., Wu, B.-W., Shi, C., Zhang, J.-H., Li, Y.-B., Tang, W.-A., Shi, T. (2013). Impacts of Urbanization and Station-relocation on Surface Air Temperature Series in Anhui Province, China. *Pure and Applied Geophysics*, *170*(11), 1969–1983. doi:10.1007/s00024-012-0619-9